

Optimal Leg Height of Landing Legs to Reduce Risk of Damage from Regolith Ejecta by Retrorocket Exhausts

Johan Karukayil¹ * , Henry Love² 

¹. Tesla STEM High School, 4201 228th Ave NE, Redmond, Washington, 98053, United States

². University of Pennsylvania, Philadelphia, Pennsylvania, 19104, United States

Email: johankarukayil@gmail.com

ABSTRACT

Over the past decade, there has been a rapid increase in rocket launches. 2022 was a record-breaking year for the aerospace industry, with 180 successful rocket launches into orbit, 44 more than the previous year. Reducing as many risks as possible is essential as interplanetary rocket launches and reusable booster landings become more frequent. One such risk occurs when a rocket/booster lands. During the landing process, the retrorockets spray debris from the loose ground, which may damage the rocket/landing module. Retrorockets are rocket engines that provide a thrust opposing the spacecraft's motion, causing it to decelerate. This paper studies the effect of landing leg height on ejecta velocity, the volume of debris ejected, and ground surface temperature change. Four landing leg heights were tested with an Estes® E-16 consumer model rocket motor: 0 mm, 50 mm, 75 mm, and 100 mm. The experiment suggests that the optimal height above the ground's surface for a simulated landing module based on the volume and velocity of the ejecta is 50 mm. Landing legs that elevate a model rocket this height create an average crater volume of 610.5 mL and a max crater diameter of 10.34 cm. After determining the optimal height, a landing leg system was developed. This system was attached to an Aerodactyl TS® model rocket and utilized landing legs that elevated the rocket to a height of 50 mm above the ground at landing.

Keywords: Engineering Mechanics; Aerospace and Aeronautical Engineering; Interplanetary Rockets; Landing Module; Retrorocket

©2023 The Authors, Published by Hyperscience International Journal. This is an open-access article under the CC BY-NC <https://creativecommons.org/licenses/by-nc/4.0/>

INTRODUCTION

The forefront of aerospace engineering is sending people to Mars. One problem that engineers are encountering is the blasting of small particles and rocks that could potentially damage payloads [1].

Currently, there are three main methods to land on Mars. The first method for smaller payloads is to lower the payload with a parachute and drop it while it is protected with airbags. The second method for mid-sized payloads is to use retrorockets and weak jetpacks. The final method is for large payloads where the payload is lowered via a set of cables from a landing module. The latter method reduces the risk of Martian regolith damaging the payload; however, it has a

high cost and is currently non-reusable. In addition, the tiny particles ejected by retrorockets can reach speeds of 2000 m/s which could dramatically damage the payload. After astronauts retrieved the Surveyor spacecraft during the Apollo mission, scientists discovered that tiny particles of about 150 microns were blasted into its various components, including the camera and other sensors [2]. Additionally, these tiny particles can damage the spacecraft's surface coatings, reflective blankets, optics, and mechanical joints. Because of this, protecting the spacecraft during landing is imperative to minimize damage. The proposed project is to study the effect of landing leg(s) height on the amount of debris ejected from a simulated Martian surface. This project

can be tested via a 2-part testing system. The first test is a functionality test which involves a stationary testing process to observe the size of the crater produced by the model rocket motor along with the velocity of the ejected particles. The second test is a flight test which implements the system onto a model rocket. Between both tests, the following data will be collected: the volume of the crater left by the rocket motor, the velocity of ejected material, and whether the landing succeeded. A comparison will be made with and without the landing system, offering insight into the best system to minimize payload damage.

METHODS

Determining Optimal Landing Leg Height

In general, the biggest obstacle to space travel and space exploration is the astronomical price. Recently, aerospace companies such as SpaceX®, Blue Origin®, Rocket Lab®, and others have started diving into reusable rocket boosters. This venture has already yielded 5 to 10 times cheaper launches than traditional rockets [3, 4]. The primary way to land rocket boosters is with retrorockets. Due to the unavailability of consumer liquid-fuel model rocket engines, traditional solid-fuel model rocket motors were used to act in place of the retrorockets [5]. The first stage of the development of the landing legs was to determine the optimal leg height above the ground. To determine the optimal height, the rocket motor was held in place at a certain height above the ground, and the velocity and volume of the ejected material were measured in addition to the surface temperature of the ground. In the experiment, sand was used as the ground material because it is mostly composed of sand [6, 7].



Figure 1: Static launch rig with temperature probes slightly exposed on the back wall in the middle of the rig. The steel beam connecting the polycarbonate visibility panel and the wooden back wall is the mounting beam for the rocket motor.

A static launch base was developed to determine the volume and ejection velocity of the sediment. This $2 \times 1 \times 1$ foot wooden box was designed with an open top, clear polycarbonate front panel, and a series of Gikfun® DS18B20 temperature probes in the back of the box to measure ground temperature. After drilling six holes, just enough to align each probe vertically with 1-inch spacing and securing a probe in each hole, the sensors were connected to an Arduino Uno®. The topmost hole is flush with the surface of the sand, resulting in the collection of ground surface temperature data.

A steel bracket that acted as a connection point for the rocket motor ran across the top of the box. This steel channel was positioned to ensure the motor was centered in the middle of the box. The motor was held in place with a custom 3D-printed piece that uses a screw-lock system. The bottom cylindrical portion of the white object in Figure 1 is a screw cap that can be unscrewed to unveil a chamber that fits a 29 mm diameter consumer model rocket motor. This experiment used an E16-0 rocket motor which can produce a total impulse of 33.68 newton-seconds of thrust and a max thrust of 26.44 newtons [8]. This body for the rocket motor is clamped to the steel beam using a standard trigger clamp. The simulated height of the landing legs can be adjusted by raising and lowering the 3D-printed piece on its flat segment. Figure 1 clearly shows the temperature probes in the box's rear, the steel support beam, and the motor clamping mechanism.

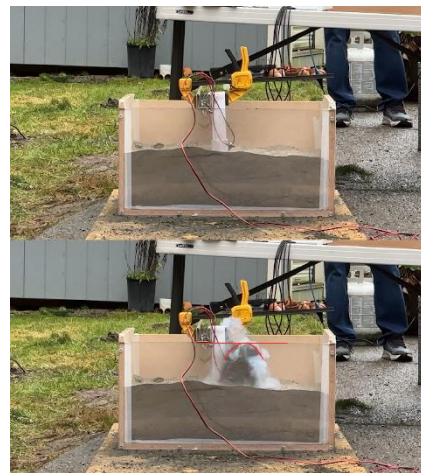


Figure 2: The time for the sand to reach the top of the polycarbonate is calculated via frame counting. As shown in the bottom image, the sand plume reached the top of the polycarbonate, marking the end time.

The box was filled with sand to the topmost temperature sensor to conduct the experiment. To conduct consistent trials, it is essential to ensure that the sand is as level as possible. After setting up the motor at the desired height above the sand (in this case, 0 mm, 50 mm, 75mm, and 100mm), the motor was connected to a standard rocketry launch controller. Before launch, a camera was set up to

record at 120 frames per second on the same level as the box in order to be able to extrapolate the velocity by frame counting using Adobe Premiere Pro. Since the distance between the top layer of sand and the topmost part of the polycarbonate panel is known, the ejection velocity of the sand can be estimated by determining the time it takes for the sand to reach the top of the polycarbonate.

To do this, the kinematic formula, $x = v_i t + 1/2 g t^2$. So that the values of x , g , and t are known. x is the distance between the surface of the sand and the top of the polycarbonate to be 13.0175 cm. G is the acceleration due to gravity which is approximately $9.8 m/s^2$. We can finally determine by frame counting the videos captured.



Figure 3: Example of one of the paraffin wax casts obtained from the experiment. The mold is upside down and hardened to show the cratering caused by the model rocket motor.

After igniting the motor, a divot formed in the sand because of the force of the motor. After a couple of minutes, standard paraffin was poured into the divot, which acted as a mold, completely filling the crater volume but not overflowing. After the paraffin wax was fully cooled, the volume and max diameter of the crater were determined. The max diameter was determined by simply using a ruler to measure the widest part of the cast. The volume was measured by filling a container to the brim with water and placing the container in another larger bucket. After slowly and carefully dropping the cast into the filled bowl, the water that spilled out the top and into the larger bowl was measured using graduated cylinders to determine the volume of the crater.

Developing Landing Legs

Determining the optimal height for landing legs is important because larger heights require longer legs and, therefore, more material. Because of this, it obviously is not scientifically and economically feasible to create extremely long legs.

After thoroughly brainstorming and designing various leg designs, the final three most promising designs were sliding legs which were locked at the lowest position, foldable

landing legs, which were flush with the rocket's body, and foldable landing legs, which protruded out of the body of the rocket. Due to the various limitations involved with model rocketry, such as the diameter of the motor, the most promising solution out of the bunch was the foldable landing legs that protruded out of the rocket's body.

Because of the additional material, it was important to build the legs with aerodynamics and weight in mind. The system was built around an Aerodactyl TS® model rocket. This 2-stage rocket was chosen due to its multistage capabilities, which could be used to unlock the legs and also mimics the multistage design of many rocket/booster designs commercially launched today.

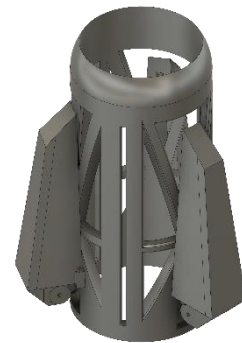


Figure 4: A 3D model of the landing leg system and bracket. The legs can pivot downwards from their original position displayed in the image. The thin vertical cutouts in the bracket are to allow fins to be slotted into it.

As shown in Figure 4, three landing legs were used. This was chosen because the rocket has 3 fins (one leg placed between each fin), and 3 points fully define a plane that prevents the rocket from “wobbling.” More than three to five legs seemed redundant and would not be a good use of materials, making the rocket more expensive and heavier.



Figure 5: A scale 3D model of the landing legs, bracket, leg locks, and model rocket. The model rocket is dark gray, the bracket is red, the legs are white, and the leg lock mechanism is black and tan. The black, red, and white portions are 3D printed out of PLA, while the tan part of the leg lock is a standard popsicle stick that has been cut. The bottom image portrays the fully deployed legs after the booster stage ejects.

There is also a triangular weight reduction pattern. Due to accessibility, a 3D printer (fused deposit modeling /fused filament fabrication) with PLA was used to create the models. The model was printed at a trihexagonal infill pattern at a 10% infill density with a 0.87 mm border thickness using a 0.15 mm layer height. This ensured a structurally strong system while also being lightweight.

The leg and bracket system are glued onto the second rocket stage. Because of this, after the first booster stage falls off, the black and brown leg locks slide off with the booster stage and unlock the now free-to-pivot legs.

The legs can then fold downwards due to the natural forces acting on them and are locked in place using a total of six $0.75'' \times 0.5'' \times 0.125''$ neodymium magnets, providing 8.5 pounds of pull force per magnet, more than enough to lock the legs open. One magnet was placed on the flat, angled portion under the leg directly to the right of the pivot, while the other magnet went in the slot in the bracket system under the pivot point of the leg. As the leg rotates downwards, these two magnets will contact and lock in place. Additionally, the leg system was designed to be modular rather than built into the rocket to ensure universality between different model rockets, as seen in Figure 5. The modularity of this system can be attributed to the fact that this bracket does not need to be glued or locked onto the model rocket since it simply goes around the fins. The legs also can be easily interchanged based on different requirements.

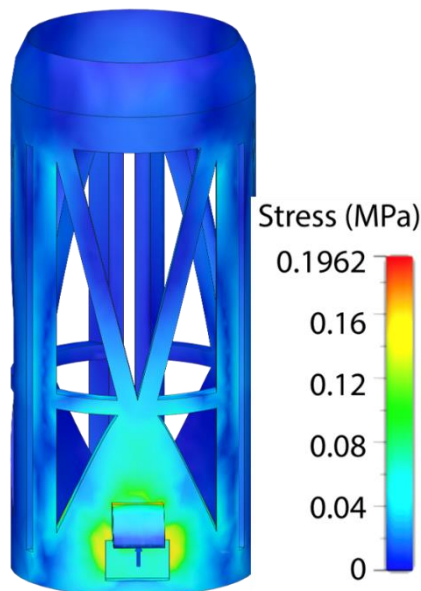


Figure 6: A finite element analysis stress visualization of the leg mount structure based on the force values determined from a model rocket simulator. Clearly, the model experiences at most about 0.17 MPa of stress.

In addition to developing a reliable leg deployment mechanism, it is important to ensure that the system is structurally stable and can withstand a landing. Using OpenRocket, a rocket simulation software, it was determined

that the total landing force was 12 newtons, meaning that each leg would independently experience 4 newtons of force. Based on this, the landing bracing was put under a finite element analysis simulation to determine how the system interacted with the forces induced by landing.

At most, the bracing would experience about 0.17 MPa of stress. Although this seems like a lot at first glance, the tensile strength of PLA plastic is 60 MPa [9]. Obviously, neither the bracing nor the legs were printed at a full, 100% infill density but rather a 10% infill density. Although significantly less material was used, the trihexagonal infill pattern significantly increased strength. This specific infill pattern has been shown to have the strongest flexural and impact strength, which are very important for this specific scenario [10]. Overall, this design is structurally stable because it can withstand over twenty times the predicted max force on the bracket.

Another important factor to consider with a rocket is its aerodynamics, both the aerodynamic stability and aerodynamic performance. OpenRocket, a model rocket software, was used to determine the aerodynamic stability because of both the shape of the general rocket, including its fins and body overall body structure, as well as the fact that the center of pressure was lower than the center of gravity the modified rocket-lander system was deemed aerodynamically stable [11].

A comparative qualitative analysis between each iteration was used to optimize the aerodynamics of the system. Autodesk Computational Fluid Dynamics 2023 software was used to determine the air velocity magnitude, surface static pressure, and static air pressure.

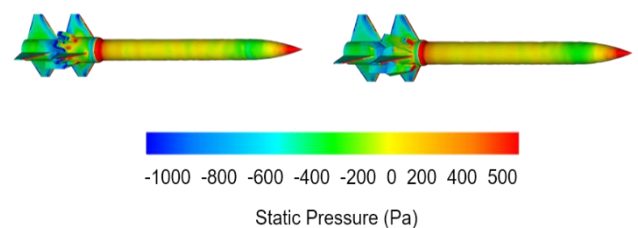


Figure 7: A computational fluid dynamics visualization of the static air pressure on the body of the model rocket. The top rocket includes the version 1 prototype bracing and legs, while the bottom rocket includes the final bracing and final leg.

The top model of the version 1 prototype clearly shows larger low-pressure zones, as depicted in blue, and also more high-pressure zones, which are depicted in red. Both pressure zones cause drag. The drag caused by high pressure is called skin drag, and the drag caused by low-pressure zones is called pressure drag. Through the various iterations of the model, the high- and low-pressure zones were decreased to reduce overall drag on the rocket. Obviously, optimizing the design to have the least drag is optimal, so it reduces fuel consumption during the launching process.

RESULTS AND DISCUSSION

Static Launch Results

From the static launch test, it was determined that the 50 mm leg height was the optimal configuration. This leg height was selected based on a combination of all the collected data, including the fact that this leg height ejected the least volume, had a low ejection velocity, and had a large crater diameter.

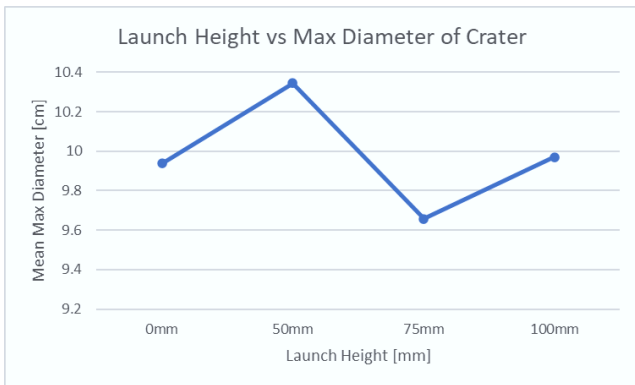


Figure 8: As the launch height increased, there was a nonlinear change in the mean max diameter.

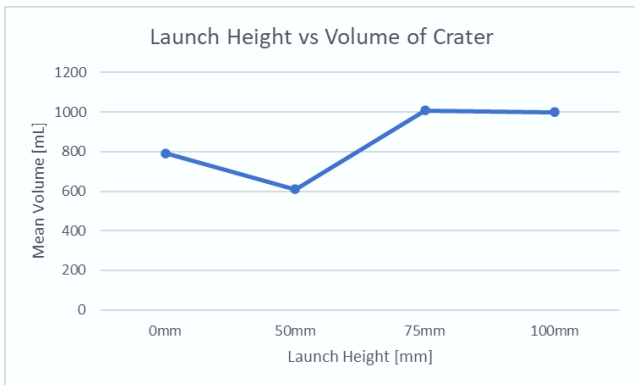


Figure 9: As the launch height increased, there was a nonlinear change in mean volumes over the 2 trials.

Table 1: Portrays the change in volume and max width of the crater produced at different launch heights.

Launch Heights	Trial No	Max Diameter (cm)	Volume (ml)
0 mm	1	9	826
	2	8.875	759
	Average	9.9375	792.5
50 mm	1	10.9375	668
	2	9.75	553
	Average	10.34375	610.5
75 mm	1	9.375	1073
	2	9.9375	944
	Average	9.65625	1008.5
100 mm	1	10.6875	996
	2	9.25	1001
	Average	9.96875	998.5

Although the 50 mm launch height produces the smallest, albeit widest, crater. This leg height ejects almost 30% less regolith than the next lowest configuration of 0 mm (Table 1). Additionally, as seen in Figure 8, the mean volume of each leg height is seemingly nonlinear, first decreasing between 0 mm and 50 mm leg heights, then increasing and flattening between 50 mm and 100mm. The max diameter of the crater, however, clearly seen in Figure 9, is inversely related to the volume, first increasing, then decreasing, and flattening out. The low ejecta volume and high max diameter of the crater indicated that the crater for the 50 mm launch height is the flattest. A flatter and less defined crater are good for Martian landings since the ground will be flatter and hence more stable.

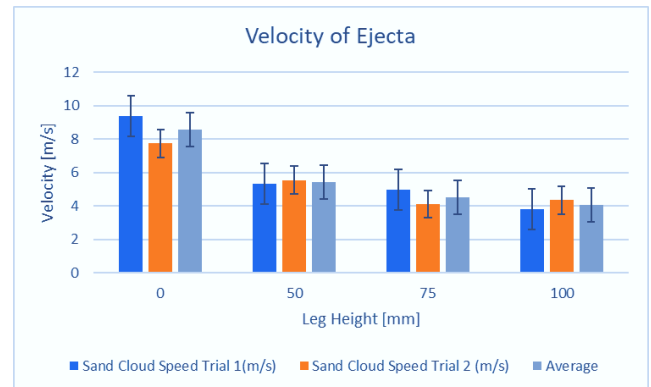


Figure 10: A visual representation of the velocity of the sand ejection at different leg heights.

When comparing the velocity of the ejecta in Figure 10, it is evident that the 0 mm leg height is by far the worst case. Although the other leg heights decrease as leg height increases, they are not statistically different because the 95% confidence intervals overlap.

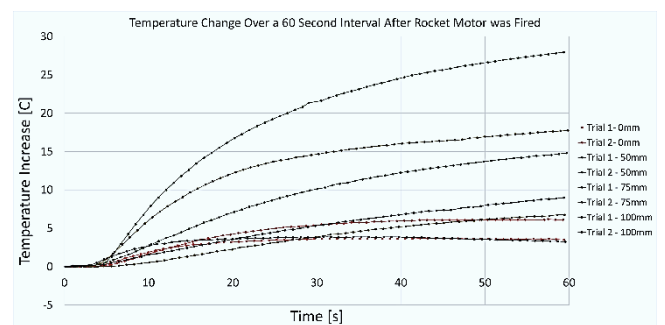


Figure 11: Portrays the change in volume and max width of the crater produced at different launch heights.

Initially, the temperature data over a 60-second interval after the motor was launched was also going to be used to determine the optimal landing leg height. After testing, however, it was clear that it became evident that the 50mm leg height led to the greatest temperature increase. This, however, could be because the temperature probe was not centered and placed directly under the motor but instead off-

centered. Additionally, because the 50 mm configuration blasted the least sand, it means that less sand will fall onto the sensor. Sand has low specific heat, meaning it can diffuse heat quickly. Because the other configurations blasted more sand, more sand would have fallen onto the sensor, cooling it down more. A paper published by NASA's Kennedy Space Center also describes a similar logarithmic trend in height and temperature increase, as observed in Figure 11 [2].

Landing Leg Test

After assembling both the model rocket and landing legs, the rocket was launched to determine the functionality of the legs. An F-class model rocket motor was used for the landing leg test launch. The launching mechanism utilized a 6-foot launch rail, which was mounted onto an off-the-shelf clamping workbench using a custom-built 3D-printed bracket. All stages of flight were completed successfully, and the entire model rocket system was able to attain a maximum altitude of 1047 feet. Although the rocket did not land perfectly back on the landing legs due to a lack of orientation control based on limitations, the legs were still able to deploy and sustain the weight of the landing.

Limitation of Landing Legs and Future Research

Building a prototype component of a rocket has its limitations. Without access to real-world materials or liquid-powered motors, this project at face value may seem inconsequential; however, these findings can still be applied to the real world. This project provides insights into the optimal leg height to minimize ejecta volume, and crater diameter, and surface temperature. Additionally, this project proposes a prototype passive leg-release mechanism that passively creates drag to slow down the descent while also being able to support the rocket upon landing.

Future research in this project could include the scalability of the study through a model. Utilizing computer simulations to study the phenomenon in the future would also increase the applicability of this research.

Sources of Error

The use of wax to determine the volume of sand is one source of error since a layer of sand, pebbles, and other debris will

be stuck to the wax. This outer layer will inflate each volume measurement by different, unequal amounts. Although minimal, this will still have an impact on the volume measurements. Another source error in determining the volume of the crater is the resettling of ejected sand. Because the wax cast could only be poured after the system had cooled, the sand that was ejected directly upwards and fell back into the crater is incorrectly characterized as material that remained in place during the launch.

Determining the velocity of the particles also may be slightly inaccurate. Because of limitations due to the framerate of cameras, the time it took for the ejecta to reach the top of the front panel comes in discrete quantities rather than exact values. This limits the resolution of the particle velocity measurement.

When it comes to observing the temperature of the crater, one potential source of error could be that the temperature probe was not directly below the rocket motor and, therefore, could return an underinflated value. Not all trials were conducted on the same day; therefore, temperature, humidity, and other weather conditions could have affected the results.

CONCLUSION

The optimal leg height for an E16 model rocket motor is 50 mm above the ground. As the landing module's height above the ground increases, the volume of the crater, max diameter of the crater, and velocity of ejecta decrease. However, an increased height implies longer legs that are heavier, weaker, and bulkier than their shorter counterparts, increasing the spacecraft's cost, range, logistics, and risks. A prototype landing leg, designed with Fusion 360 and made primarily with PLA with neodymium magnetic clamps, was successfully able to elevate the model rocket to the appropriate height above the ground.

AUTHORS

My name is Johan Karukayil, and I am a high schooler interested in Aerospace Engineering. As a passionate young aerospace engineer, I hope to work on NASA's Artemis missions in the future to help take people to Mars. To achieve my dream, I plan to get a master's degree in aerospace engineering.

REFERENCES

- [1] C. M. Donohue, P. T. Metzger, and C. D. J. a. p. a. Immer, "Empirical Scaling Laws of Rocket Exhaust Cratering," 2021.
- [2] P. T. Metzger *et al.*, "Cratering of Soil by Impinging Jets of Gas, with Application to Landing Rockets on Planetary Surfaces," 2021.
- [3] B. Wang. (2022). *SpaceX reusable rocket costs versus airplanes.* Available: <https://www.nextbigfuture.com/2022/02/spacex-reusable-rocket-costs-versus-airplanes.html>
- [4] A. J. N. Witze, "2022 was a record year for space launches," *Nature News*, 2023.

- [5] (2023). *Apogee Components, I. Rocket Propulsion*. Available: <https://www.apogeerockets.com/Rocket-Propulsio>
- [6] (2021). *Soil on Mars. Let's Talk Science*. Available: <https://letstalkscience.ca/educational-resources/backgrounders/soil-on-mars>
- [7] G. W. Wamelink, J. Y. Frissel, W. H. Krijnen, M. R. Verwoert, and P. W. J. P. O. Goedhart, "Can plants grow on Mars and the moon: a growth experiment on Mars and moon soil simulants," vol. 9, ed, 2014, p. e103138.
- [8] *E16-0 engines (29 mm). Estes Rockets*. . Available: <https://estesrockets.com/products/e16-0-engines>
- [9] J. A. Travieso-Rodriguez, R. Jerez-Mesa, J. Llumà, O. Traver-Ramos, G. Gomez-Gras, and J. J. J. M. Roa Rovira, "Mechanical properties of 3D-printing polylactic acid parts subjected to bending stress and fatigue testing," vol. 12, ed, 2019, p. 3859.
- [10] G. Y. Dakhil, R. M. Salih, and A. M. Hameed, "The influence of infill pattern and infill density on the (tensile, flexural and impact) strength of 3D printed polymers," in *AIP Conference Proceedings* vol. 2660, ed: AIP Publishing, 2022.
- [11] NASA. (2023). *What is lift?*. NASA. Available: <https://www1.grc.nasa.gov/>